Macromolecular Rapid Communication
www.mrc-journal.de

Reconfigurable Soft Actuators with Multiple-Stimuli Responses

*Tonghui Zhao, Wenchao Dou, Zhiming Hu, Wenhao Hou, Yirui Sun, and Jiu-an Lv**

Multiple-stimuli responsive soft actuators with tunable initial shapes would have substantial potential in broad technological applications, ranging from advanced sensors, smart robots to biomedical devices. However, existing soft actuators are often limited to single initial shape and are unable to reversibly reconfigure into desirable shapes, which severely restricts the multifunctions that can be integrated into one actuator. Here, a novel reconfigurable supramolecular polymer/polyethylene terephthalate (PET) bilayer actuator exhibiting multiple-stimuli responses is presented. In this bilayer actuator, the supramolecular polymer layer constructed of poly(5-Norbornene-2-carboxylic acid-1,3-cyclooctadiene) (PNCCO) and azopyridine derivative (PyAzoPy) via H-bonds provides multiple-stimuli responses: PyAzoPy offers light response and carboxylic groups in PNCCO endow the actuator with humidity response. Meanwhile thermoplastic PET layer enables the bilayer actuators to be reconfigured into various shapes by thermal stimuli. The rationally designed actuators exhibit versatile capabilities to reversibly reconfigure into a set of initial shapes and carry out multiple functions, such as photo-driven "foldback-clip" and Ω-shaped crawling robots. In addition, bio-inspired plants constructed by reconfiguration of such actuators demonstrate reversible multiple-stimuli responses. It is anticipated that these novel actuators with highly tunable geometries and actuation modes would be useful to develop multifunctional devices capable of performing diverse tasks.

Actuators constructed by intelligent materials are capable of transforming external stimulus such as light, temperature, humidity, magnetic field and electricity into mechanical stress leading to various structural shapes and surprising movements especially on polymeric actuators.[1–14] Many polymer systems have been exploited as soft actuators for instance hydrogels, shape-memory polymers and liquid crystalline polymers etc. which enable multiple stimuli-responses,[15–17] and are promising to be developed as sensors, soft robotics, artificial muscle and microfluidic systems.[18–24]

However, for soft actuators previously reported, limited morphology and single actuation extremely restrict them to execute multifunctions.[21–24] Therefore, developing soft actuators capable of reconfiguration into anticipant initial structural shape and reversible actuation by multi-stimuli would increase potential applications, more importantly, also alleviate the restrictions in design and freedom of actuators. For shape reconfiguration, reversible reprocessing the same actuators into diverse shapes is generally achieved through dynamic crosslinking structures which can be thermally induced bond exchange and structurally reconstruct under external stress.[25,26] Additionally, reconfigurable strategy relying on a reverse patterning was also conducted in previous reports,[27,28] which could encode and erase prescribed 3D geometric information reversibly. Zhao's group provided a thermal programming method that used the bilayer actuator composed of LCN and polyimide to process it into various "Janus" structured soft robots, which could be easily reprocessed into various 3D shape capable of diversiform motions.[29] Recently, Schenning and co-workers showed a thermoplastic bilayer actuator consisting of polyethylene terephthalate (PET) and LCN.[30] Through thermal-induced shape programming, the actuator can be re-shaped from folded geometries into more classical bent or helical shape actuators, opening a door to facilely prepare shape-reconfigurable actuators.

Supramolecular polymer, whose components can be bridged via reversible noncovalent crosslinking and take continuous assembly/disassembly processes under specific conditions,[31–35] have been emerging as smart materials for soft actuators presenting diverse properties such as shape-memory, folding, bending and self-healing etc. triggered by temperature, light, chemistry and so on.[36–44] For most photoresponsive supramolecular polymers, the azobenzene (azo) dyes and its derivatives are usually essential, and provide *trans–cis* photoisomerization

T. Zhao, Z. Hu, W. Hou
School of Materials Science and Engineering
Zhejiang University
Hangzhou 310027, China

T. Zhao, Dr. W. Dou, Z. Hu, W. Hou, Y. Sun, Dr. J.-a. Lv
Key Laboratory of 3D Micro/Nano Fabrication and Characterization of Zhejiang Province, School of Engineering
Westlake University
18 Shilongshan Road, Hangzhou, Zhejiang Province 310024, China
E-mail: lvjiuan@westlake.edu.cn

T. Zhao, Dr. W. Dou, Z. Hu, W. Hou, Y. Sun, Dr. J.-a. Lv
Institute of Advanced Technology
Westlake Institute for Advanced Study
18 Shilongshan Road, Hangzhou, Zhejiang Province 310024, China

The ORCID identification number(s) for the author(s) of this article can be found under https://doi.org/10.1002/marc.202000313.

DOI: 10.1002/marc.202000313

© 2020 Wiley-VCH GmbH

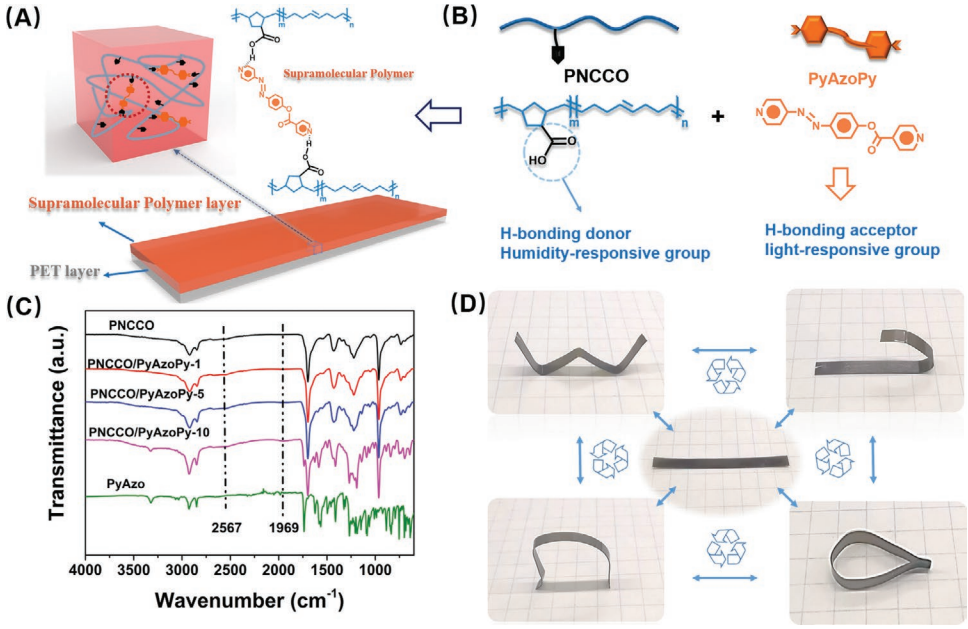

Figure 1. Design of reconfigurable soft actuators with multiple-stimuli responses. A) Schematic illustration of the structure of supramolecular polymer/PET bilayer actuator. B) Chemical structures of PNCCO and PyAzoPy, which were used to construct the supramolecular polymer via multiple hydrogen bonds. C) ATR–FTIR spectra of PNCCO, PyAzoPy, and PNCCO/PyAzoPy networks. D) Shape reconfiguration of the bilayer actuator. The shapes of supramolecular polymer/PET bilayer actuator were reconfigured by manually folding the actuator at 140 °C and following fixed at room temperature. The size of the bilayer actuator is 40 mm × 3 mm × 0.13 mm.

that leads to bending actuation.[45,46] Therefore, incorporating azo group into polymer is an effective and facile approach to construct light-responsive supramolecular.[35,46–48] Si et al. showed hydrogen-bonded supramolecular assembly with t-Azo and PAA-u.[47] The isomerization of t-Azo crosslinkers induces bending deformation and shape recovery under external light stimuli. Feng prepared an electrostatic interaction supramolecular assemble H4abtc/PDAC.[48] The free-standing H4abtc/PDAC film shows excellent light-, humidity-, and heat-response and exhibits a large shape deformation. Additionally, Qin et al. prepared light-driven flexible actuators based on electrostatic interaction of supramolecular assembly using crosslinked AZZO/PDAC, and the supramolecular actuators exhibited a large deformation by rolling-up into a tube upon UV irradiation.[35]

For polymer/azo supramolecular systems, azopyridine derivatives usually act as crosslinker to form multiple-stimuli responsive supramolecular polymers, in which they not only help to construct intermolecular hydrogen bonds between carboxyl and pyridyl moieties, but also provide light-responsive feature brought by the reversible photoisomerization of azo groups.[46,49] Ikeda and co-workers showed a kind of supramolecular liquid crystalline assembly by intermolecular hydrogen bonding.[46] The *tans–cis* photoisomerization of the azobenene moieties cause macroscopic deformation of polymer films. Supramolecular complex containing azopyridine derivative provide a promising material to construct smart supramolecular actuators. In addition, for advanced materials, to fabricate composites usually compensate for insufficient on functions for instance bilayer actuators.[12,13,30,50,51]

Herein, we report a reconfigurable supramolecular polymer/PET bilayer actuator with multiple-stimuli responses. The supramolecular polymer is constructed through incorporation of azopyridine derivatives (PyAzoPy) into copolymer (PNCCO) using multiple H-bonds. Thermoplastic PET enables the actuator to reconfigure into different initial shapes. Through shape-reconfiguration by heating, various actuators have been designed, and they are capable of transforming diverse deformations, exhibiting light, thermal, and humidity responses. This work presents a facile and high freedom method for creating multiple functional actuators.

In this work, we fabricated a novel hierarchical-structured actuator consisted of two functional layers: supramolecular polymer layer and thermoplastic PET layer as shown in **Figure 1**A. The former layer endows the actuators with multiple responses, while the latter layer provides shape reconfiguration and mechanical robustness. The supramolecular layer made of PNCCO/PyAzoPy employs multiple intermolecular H-bonds to form 3D network structure, and the chemical structures of PNCCO (H-bonding donor) and PyAzoPy (H-bonding acceptor) as shown in Figure 1B. Multiple hydrogen bonds are versatile intermolecular interaction used to effectively construct supramolecular polymers.[47,52] The azopyridine derivatives PyAzoPy as crosslinker contains two pyridine groups as hydrogen-bond acceptors, which can form multiple H-bonds with carboxyl group (hydrogen-bond donor) on PNCCO chains. The multiple intermolecular H-bonds in PNCCO/PyAzoPy network are characterized by Fourier-transform infrared spectroscopy (FTIR) and dissolving experiments. As shown in Figure 1C, two additional peaks at 2567 and 1969 cm^{-1} appear in the FTIR spectra of PNCCO/PyAzoPy complexes, which can be assigned to the Fermi resonance bands and the vibration of hydroxyl groups, respectively.[53] Compared with neat PNCCO

© 2020 Wiley-VCH GmbH

and PyAzoPy, the peaks of the supramolecular network are getting higher and somewhat broaden as the increasing content of crosslinker PyAzoPy, strongly indicating that more H-bonds are formed between the carboxylic group of PNCCO and the pyridyl group of PyAzoPy,[53,54] which can lead to an increase of H-bonding density of the network in the matrix. Moreover, the formation of multiple H-bonds is also further confirmed by dissolution testing, as revealed in Figure S2 in the Supporting Information. Supramolecular PNCCO/PyAzoPy is insoluble in several solvents such as ethyl alcohol, ethyl acetate, but which can completely dissolve PyAzoPy. It is noted that, for neat PNCCO copolymer, there are many carboxylic groups in molecular chains, and the carboxylic side chains dimerized by noncovalent H-bonds can efficiently crosslink macromolecular chains forming noncovalent network. Therefore, neat PNCCO copolymer can construct supramolecular network forming through self-complementary hydrogen bonding units of crosslinked point carboxylic acids similar like previous report.[55]

The effects of multiple H-bonds on thermal and mechanical properties of PNCCO/PyAzoPy complexes were investigated. According to differential scanning calorimetry (DSC) measurement shown in Figure S3 in the Supporting Information, the Tgs of samples present a downtrend, possibly resulting from the addition of PyAzoPy molecules which enhance movement of macromolecular chain segments and the flexibility of polymer.[56] As shown in Figure S4 in the Supporting Information, neat PNCCO exhibits lower elongation at break and higher Young's modulus, owing to the higher strength of H-bonding interaction between molecular chains. Although the Young's modulus and tensile strength of PNCCO/PyAzoPy-1 decreases owing to the enhanced movement of macromolecular chains of PNCCO through incorporation of small molecule of PyAzoPy, the tensile toughness improved significantly comparing to neat PNCCO. Detailed tensile data are provided in Table S1 in the Supporting Information, which shows that tensile strength, Young's modulus and elongation at break of PNCCO/PyAzoPy samples are enhanced with the increasing content of crosslinker PyAzoPy, attributing to the enhanced multiple H-bond effect induced by increasing the content of PyAzoPy, indicating that supramolecular polymer perform superior mechanical properties. Moreover, the photochemical properties of PNCCO, PyAzoPy, and PNCCO/PyAzoPy films were also investigated by UV–vis absorption spectroscopy, as shown in Figure S5 in the Supporting Information. Upon 365 nm UV irradiation (Figure S5A, Supporting Information), the stable elongated *trans* configuration of the PyAzoPy molecule transformed into a bent *cis* configuration, demonstrated by a decrease in the intensity of the π–π^* absorption band at 342 nm of the *trans*-isomer and an increase in the n–π^* band absorption at 450 nm of the *cis*-isomer, indicating the isomerization of PyAzoPy under UV irradiation.[46] Comparing to neat PNCCO and PyAzoPy, the absorption wavelength of PNCCO/PyAzoPy films have significantly red-shifted, possibly on account of forming multiple H-bonds. The isomerization of azopyridine moieties have been widely observed in previous polymer/azo photo-responsive systems, inducing photodeformation of the polymer/azo films.[46,51] Generally, photoisomerization of the azobenzene/azopyridine derivatives moieties partly breaks the hydrogen-bonds of supramolecular, leading to volume expansion of the azobenzene/azopyridine derivatives-containing polymer and thus causes to the bending of the film actuator. The light-induced expansion effect of azobenzene/azopyridine derivatives-containing polymers have been proved by previous reports.[6,7,46] As shown in Figure S6A in the Supporting Information, the light-driven bending of PNCCO/PyAzoPy complex films are characterized under UV light with different intensity. The bending angle of PNCCO/PyAzoPy-1 film can be enhanced through increasing the incident intensity. Furthermore, PNCCO/PyAzoPy complex film with higher content of crosslinker exhibits larger bending angle upon light irradiation (Figure S6B, Supporting Information), presenting dramatically enhanced photodeformation.

To gain shape-reconfiguration feature, PET film was stuck on the supramolecular polymer film to form PET/supramolecular bilayer actuators. Thermoplastic PET capable of remolding under heating allow it to be reprocessed into any desired permanent shapes.[30] Meanwhile, PET with high Young's modulus and tensile strength (Table S2, Supporting Information) is suitable to enhance mechanical robustness of soft actuators.[30] Integrating thermal plasticity and robustness of PET, the bilayer actuator shows a shape reprogrammable characteristic at high temperature. Through recyclable shape reconfiguration, we obtained various structural actuators from one sample, such as foldback-clip-shaped and Ω-shaped actuators as shown in Figure 1D. The opening and closing of the foldback-clip-shaped actuator was controlled by switching on and off UV as shown in **Figure 2**A and Movie S1 in the Supporting Information. Figure 2B shows the schematic illustration of photo-induced reversible opening of such actuator. The Ω-shaped actuator exhibited crawling locomotion driven by UV light as shown in Figure 2C. Figure 2D schematically illustrates its crawling mechanism. The foreleg of the "crawler" bends and pulls forward under UV stimulation, while the back-leg pushes backward after UV off, making "crawler" move forward (Movie S2 in the Supporting Information). Moreover, our actuators also present temperature response, as shown in Figure S9 in the Supporting Information. The reprogrammed "foldback clip" and "arch" shaped actuators opened under 80 °C (temporary shape) and then closed to recover its original structure after cooling to room temperature, attributing to the shape memory effect of PET film. For soft actuators, self-healing is significantly important for improving robustness. As shown in Figure S10 in the Supporting Information, the bilayer actuator was cut to generate scratch with a depth about 10–30 μm on supramolecular layer using a razor blade. After annealing for 1 min at 80 °C, self-healing of bilayer actuator was pronounced significantly, deriving from the reversible interaction of multiple H-bonds favoring the interactions among polymer chains at a high temperature for supramolecular polymer.[44,57] For supramolecular polymers, self-healing can be activated at high temperature because of the relatively free movement of macromolecular chains favors the re-forming of hydrogen bonds.[58,59] The bending rate and angle could be controlled by changing the intensity of incident light, as shown in Figure 2E, showing that bending angle and rate can be considered as a sensor of intensity of radiation. It can be obtained that the high-intensity irradiation of UV facilitates fast and larger deformation for the bilayer actuators. Moreover, to figure out how

© 2020 Wiley-VCH GmbH

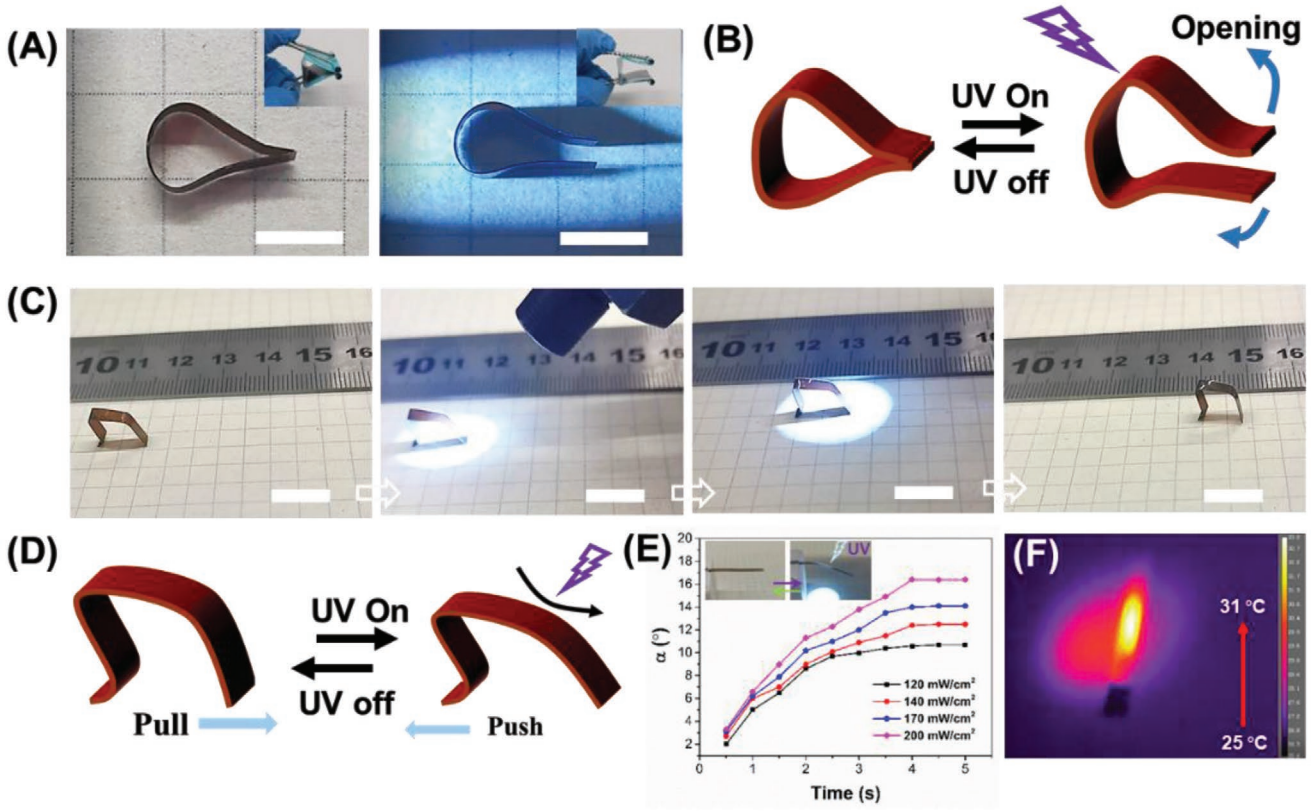

Figure 2. Photo-driven "foldback clip" and Ω-liked shape actuator. A) Photographs showing light (365 nm, 150 mW cm^{-2}) induced opening (UV on, right) and closing (UV off, left) of the "foldback clip" actuator. The scale bar is 0.5 cm. B) Schematic illustration of the photo-driven reversible opening and closing of "foldback clip" actuator. C) Photographs exhibiting light-induced walking of the Ω-liked shape actuator (365 nm, 150 mW cm^{-2}). The scale bar is 1.0 cm. D) Schematic illustration of the photo-driven walking mechanism of the crawler. E) Time-dependent bending angles when irradiated upon UV with different intensities. The inset shows light-induced bending of the actuator. The size of the actuator is 40 mm × 3 mm × 0.13 mm. F) The infrared thermal image of the actuator upon UV irradiation (365 nm, 150 mW cm^{-2}).

the structure of the bilayer actuator influences its photoresponsive behaviors, we further investigated the photoinduced bending angle of several bilayer actuators with varied thickness of the supramolecular layer. As shown in Figure S8 in the Supporting Information, when the thickness of the PET layer was fixed at 60 µm, the photo-induced bending angle of the actuators increased as the thickness of the supramolecular layer was changed from 60 to 160 µm. In agreement with earlier studies,[11,14] the investigation suggests that a thicker supramolecular layer would enhance the photo-induced bending behavior of the bilayer actuator, and the photoinduced driving force should be proportional to the thickness of the supramolecular layer. The bending of the bilayer actuator also arises from the photoinduced volume expansion of the azopyridine-containing supramolecular layer: UV irradiation causes the volume expansion of the photoactive supramolecular layer and induces stress within a short period between the supramolecular layer and the PET layer, and thus the stress leads to the bending of the bilayer actuator. For these bilayer actuators, they always reversibly bend towards the PET layer side independent of the incident direction of UV light (Scheme S1, Supporting Information). The light-induced expansion effect of azopyridine-containing polymers have been also proved by previous reports.[6,7,46] To evaluate whether UV irradiation generate amount heat and result in bending deformation of bilayer actuators, we performed the experiment of thermal imaging as shown in Figure 2F. It is clearly indicated that the temperature of the actuator only increased by 6 °C and then kept stability after UV irradiation for 3 s, suggesting photo-thermal effect could be ignored and the isomerization of PyAzoPy is dominant to induce the deformation of the actuators.[46]

Multiple-stimuli responsive materials show promising applications in biomimetic materials.[60] Besides light and temperature response, the bilayer actuator shows humidity responsive ability (**Figure 3** and Scheme S2, Supporting Information). The supramolecular surface of bilayer actuators was treated with 0.1 mol L^{-1} NaOH aqueous solution for 15 min, as shown in Figure 3A. The carboxylic acid groups on the surface of the supramolecular layer were neutralized and converted into amount of hygroscopic carboxylic salts ($COO^{-}Na^{+}$).[61] When the relative environmental humidity increases, water molecules permeate into the supramolecular polymer and increase free volume generating a tensile force, thus leading to the expansion of supramolecular polymer layer. On the contrary, when the environmental humidity decreases, water molecules evaporate, and then an extrusion force is generated, causing the shrinkage of supramolecular polymer layer.[62] Therefore, when the absorption and desorption are dynamically undergoing on

© 2020 Wiley-VCH GmbH

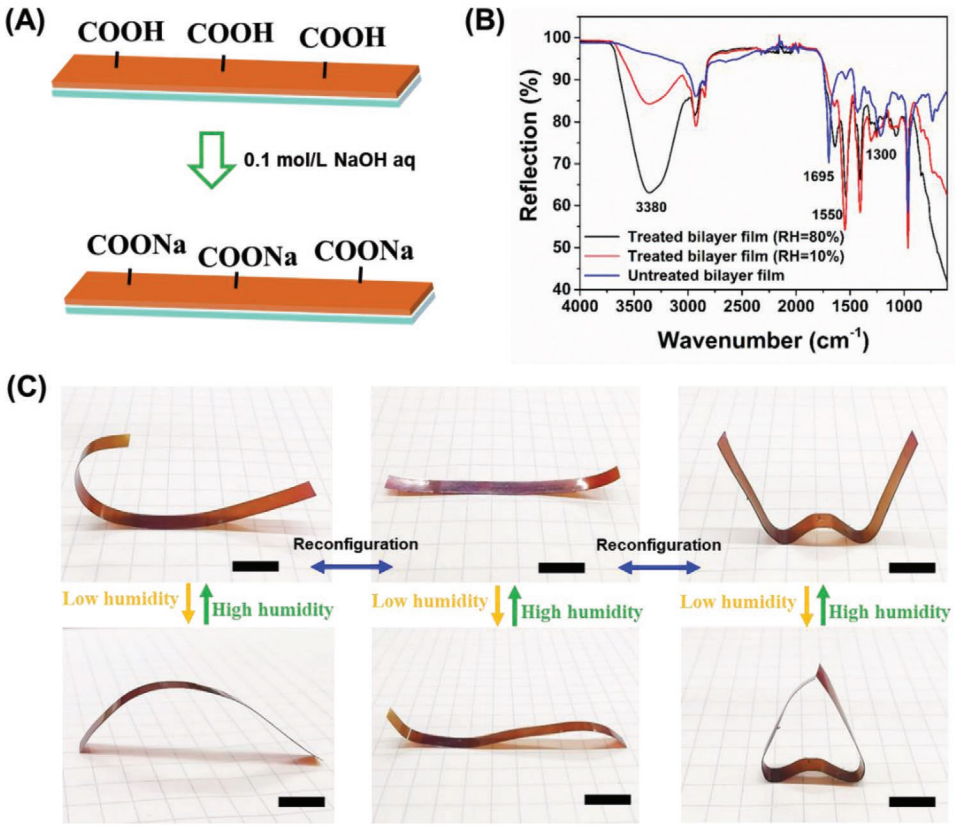

Figure 3. Humidity response of the actuators. A) Schematic illustration of switching on humidity response through surface treatment of the supramolecular layer with 0.1 mol L^{-1} NaOH aqueous solution for 15 min obtaining hygroscopic surface, resulting the reversible bending of bilayer film when alternately exposed to wet and dry environment. B) Comparisons of ATR–infrared reflectance spectra among treated bilayer films placed in different humidity and untreated bilayer film. C) Actuators with various reconfigured shapes undergo reversible deformation by high (80%) and low humidity (10%). The scale bar is 1.0 cm.

the top of supramolecular polymer surface, the bilayer actuators will bend reversibly. Figure S12 in the Supporting Information demonstrates the time-dependent bending angles induced by low (10%) and high humidity (80%) for NaOH-treated bilayer actuator, indicating that the bending angle and rate can be considered as a sensor humidity sensor. In addition, we investigated the differences of the photo-induced bending performance of the actuator before and after 0.1 mol L^{-1} NaOH aqueous solution treatment. As shown in Figure S11A in the Supporting Information, the actuator showed ≈12° bending upon UV irradiation before the treatment while it bent ≈16° after the treatment. To figure out why the treatment induces the increase of the bending angle, we performed the tensile test of the actuator and the supramolecular polymer (PNCCO/PyAzoPy) before and after the treatment, respectively. As shown in Figure S11B in the Supporting Information, the treatment leads to the decrease in the elastic modulus from 1460 to 994 MPa for the bilayer actuator, and from 410 to 118 MPa for the supramolecular polymer. These results suggest that the treatment can soften the supramolecular layer of the bilayer actuator, making it bend more easily upon UV irradiation.

To identify structure changes during the treatment, ATR–FTIR reflectance spectra of untreated bilayer film and treated bilayer film in environments with different relative humidity are shown in Figure 3B. Untreated bilayer film shows a peak around 1695 cm^{-1}, which corresponds to hydrogen-bonded carboxylic acid. Whereas the characteristic peaks almost disappear in spectra after being treated by NaOH and two new peaks appear at around 1550 and 1300 cm^{-1}, due to antisymmetric and symmetric COO^- stretching.[61] Moreover, characteristic peak of H-bonds of supramolecular at 2567 cm^{-1} disappears, sufficiently indicating that hydrogen bonds have been broken and carboxylic salt is formed. From ATR–FTIR reflectance spectra, in addition, when the treated bilayer film is exposed to varied humidity condition, the stretching vibration band (OH) at 3380 cm^{-1} under wet condition becomes larger than dry condition for treated bilayer film, further suggesting the effects of the water adsorption and desorption on structural changes of bilayer film.[62]

As expected, by thermal reconfiguration, various shape architectures were obtained such as letter-like shapes "I," "J," and "W," and those structural actuators presented different humidity-responsive properties by changing shapes depending on bending or expanding reversibly under low and high humidity as shown in Figure 3C. Finally, an artificial flower was built and exhibited reversible opening (**Figure 4**B) and closing (Figure 4A) under relative 80% and 10% humidity, respectively (Movie S3, Supporting Information). To demonstrate the synergistic effects of light and humidity, a biomimetic "two leaved clover" was fabricated with treated bilayer film as

© 2020 Wiley-VCH GmbH

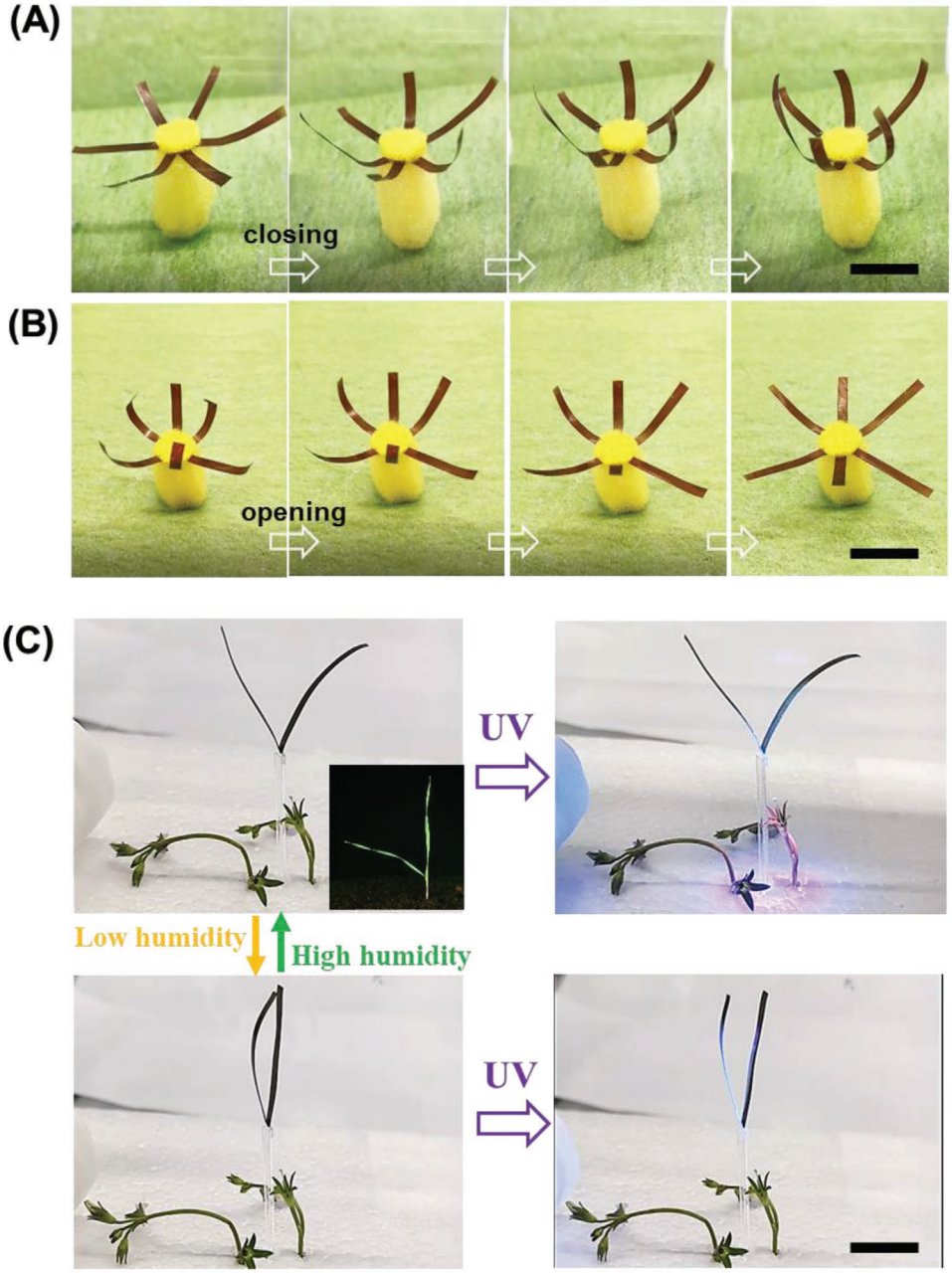

Figure 4. Bio-inspired plant exhibiting multiple-stimuli responses. Bio-inspired flower consisted of six actuators shows reversible closing A) and opening B) under relative humidity of 10% and 80%, respectively. C) Light and humidity responses of bio-inspired two-leaves grass. Two leaves open slowly under wet and the opened angle can be enlarged by UV stimuli. On the contrary, the "two leaved clover" closes under dry and can be opened by UV light. The inset shows the real grass with two leaves in nature. The scale bar is 1.5 cm.

shown Figure 4C. The leaves opened under wet environment and the opened angle would be enlarged by UV. Conversely, the leaves then closed when relative humidity decreased. But, no matter how dry the environment is, it could still be opened upon UV irradiation, exhibiting reversible and dynamical morphing through multiple stimuli, which is essential for intelligent actuators.

In summary, reconfigurable hierarchical-structured actuators with multiple responses was rationally designed and prepared with functional supramolecular polymer and thermoplastic PET. The multiply responsive supramolecular polymer was constructed with copolymer PNCCO and azopyridine derivative PyAzoPy via multiple intermolecular H-bonds. Combining thermal plasticity and robust mechanical properties of PET, the hierarchical-structured actuator presents shape-reconfiguration ability which enable researchers to endow the actuators with desirable function through remolding soft actuator into desired initial shape. In this report, the designed actuator was reconfigured into diverse shapes, and can be driven by UV light, thermal, or humidity. It can function as a smart "foldback-clip"

© 2020 Wiley-VCH GmbH

or serve as a crawling robot remotely controlled through UV irradiation. Interestingly, our actuators show the capabilities to be reprocessed into bio-inspired plants that are synergistically responding to environmental stimuli (humidity and light). It is anticipated that such reconfigurable soft actuators with multiple-stimuli responses would be used to develop smart robotics and sensors with the capability of performing multi-functions.

Experimental Section

Materials: 5-Norbornene-2-carboxylic acid, 1,3-cyclooctadiene and second-generation Grubbs catalyst were purchased from Adamas and used without further purification. PyAzoPy was synthesized according to previous report.[51] The commercialized PET tape with the thickness of 60 μm was purchased from Angulaobao Co. Ltd. Dichloromethane and tetrahydrofuran were obtained from Greagent, and dichloromethane was dried over calcium hydride under N_2 gas protection and then distilled before use. Other reagents were used as received.

Synthesis of Copolymer PNCCO: The synthetic rout of copolymer PNCCO is shown in Figure S1 in the Supporting Information. The solution of 5-Norbornene-2-carboxylic acid (2 g) and 1,3-cyclooctadiene (1.57 g) in dry CH_2Cl_2 (15 mL) was placed into a Schenk flask (25 mL). After the solution was degassed by freeze-pump-thaw cycles for three times, second generation Grubb's catalyst (24.58 mg) in 2 mL of degassed CH_2Cl_2 was injected into the Schlenk flask by syringe under nitrogen atmosphere. The mixture was stirred at room temperature for 12 h. Finally, the brown precipitates were collected and then dried under vacuum. The molecular weight M_n and M_w of copolymer were 26 and 33 kDa, respectively, characterized by APC. ^{1}H-NMR (500 MHz, THF-d8): δ (ppm) 10.36 (broad), 5.25 (broad), 3.05 (broad), 2.75 (m), 2.37 (broad), 1.92 (m), 1.30 (broad).

Preparation of Supramolecular Complexes: After the addition of crosslinker PyAzoPy with different weight ratio (0, 1, 5, 10 wt%) to a solution of the copolymer PNCCO (2 g) in THF (20 mL), the solution was stirred for two days and then the solvent was evaporated slowly under vacuum to give final supramolecular complex PNCCO/PyAzoPy-*x*, where *x* denotes as the weight ratio of PyAzoPy.

Preparation and Reconfiguration of Bilayer Film Actuators: The synthesized copolymer was hot-pressed into a thin film about ≈60 μm at 160 °C. Then, PET tape was pasted on one side of copolymer surface, forming bilayer film with thickness of ≈130 μm. The bilayer film was then cut into proper sizes ($40 \times 3 \times 0.13$ mm^3) and ready for reconfiguration. The obtained bilayer film was manually folded into corresponding shapes on hot stage at 140 °C, then removed from hot stage and fixed its shapes at room temperature. With no other notes, supramolecular complex PNCCO/PyAzoPy-1 was used to prepared actuators in this work. For bilayer actuators "foldback-clip" and Ω-shaped crawling robots, PET layer was outside and supramolecular layer was exactly inside.

Characterizations: The molecular weight of copolymer PNCCO was characterized by ACQUITY advanced polymer chromatography (APC) with refractive index (RI) detection at 40 °C. THF as mobile phase flowed with a rate of 0.4 mL min^{-1}. FTIR spectroscopy was carried out on a Thermo Scientific Nicolet iS50 (America). ^{1}H-NMR spectra were obtained on an AVANCE NEO 500 MHz spectrometer with THF-d8 as solvent and trimethylsilyl as an internal standard. The DSC measurement was carried out by a TA Instruments DSC250 with a heating rate of 10 °C min^{-1} in a nitrogen atmosphere. The UV–vis absorption spectra of PNCCO/PyAzoPy complex films were recorded using a Shimadzu UV-2700 spectrophotometer. Infrared thermal imager instrument (FLIR-A600-Series, Sweden) was used to observe photothermal effect. Tensile test of supramolecular was carried out using an Instron 5943 instrument at a crosshead speed of 5 mm min^{-1} at room temperature. The UV light-induced bending of the actuators was performed using OMRON ZUV-C30H LED UV light, and the intensity of UV light was measured by optical power meter (HIOKI3664, Japan). The humidity-response properties of the actuators were observed in two enclosed environments with relative humidity 10% (low humidity) and 80% (high humidity), respectively.

Supporting Information

Supporting Information is available from the Wiley Online Library or from the author.

Acknowledgements

This research was supported by Foundation of Westlake University, National Natural Science Foundation of China (51873197), and 151 Talent Project of Zhejiang Province.

Conflict of Interest

The authors declare no conflict of interest.

Keywords

hydrogen bonds, multiple-stimuli responses, reconfiguration, supramolecular actuators, thermoplasticity

Received: June 9, 2020
Revised: July 20, 2020
Published online:

[1] H. W. Huang, F. E. Uslu, P. Katsamba, E. Lauga, M. S. Sakar, B. J. Nelson, *Sci. Adv.* **2019**, *5*, 1532.
[2] X. B. Ji, X. C. Liu, V. Cacucciolo, M. Imboden, Y. Civet, A. El Haitami, S. Cantin, Y. Perriard, H. Shea, *Sci. Rob.* **2019**, *4*, 6451.
[3] C. Y. Ahn, X. D. Liang, S. Q. Cai, *Adv. Mater. Technol.* **2019**, *4*, 1900185.
[4] P. Boyraz, G. Runge, A. Raatz, *Actuators* **2018**, *7*, 48.
[5] L. X. Lyu, F. Li, K. Wu, P. Deng, S. H. Jeong, Z. G. Wu, H. Ding, *Natl. Sci. Rev.* **2019**, *6*, 970.
[6] O. S. Bushuyev, M. Aizawa, A. Shishido, C. J. Barrett, *Macromol. Rapid Commun.* **2018**, *39*, 1700253.
[7] X. Li, S. Ma, J. Hu, Y. Ni, Z. Lin, H. Yu, *J. Mater. Chem. C* **2019**, *7*, 622.
[8] M. Medina-Sanchez, V. Magdanz, M. Guix, V. M. Fomin, O. G. Schmidt, *Adv. Funct. Mater.* **2018**, *28*, 1707228.
[9] H. B. Wang, M. Totaro, L. Beccai, *Adv. Sci.* **2018**, *5*, 1800541.
[10] X. Cheng, Y. H. Zhang, *Adv. Mater.* **2019**, *31*, 1901895.
[11] J. Hu, X. Li, Y. Ni, S. Ma, H. Yu, *J. Mater. Chem. C* **2018**, *6*, 10815.
[12] S. Ma, X. Li, S. Huang, J. Hu, H. Yu, *Angew. Chem.* **2019**, *131*, 2681.
[13] X. Li, S. Ma, J. Hu, Y. Ni, Z. Lin, H. Yu, *J. Mater. Chem. C* **2019**, *7*, 622.
[14] Z. Liu, R. Tang, D. Xu, J. Liu, H. Yu, *Macromol. Rapid Commun.* **2015**, *36*, 1171.
[15] A. Kotikian, C. McMahan, E. C. Davidson, J. M. Muhammad, R. D. Weeks, C. Daraio, J. A. Lewis, *Sci. Rob.* **2019**, *4*, 7044.
[16] S. J. Chen, F. N. Mo, S. G. Chen, Z. C. Ge, H. P. Yang, J. D. Zuo, X. K. Liu, H. T. Zhuo, *J. Mater. Chem. A* **2015**, *3*, 19525.
[17] R. X. Liang, H. J. Yu, L. Wang, L. Lin, N. Wang, K. U. R. Naveed, *ACS Appl. Mater. Interfaces* **2019**, *11*, 43563.
[18] Y. L. He, S. L. Liao, H. Y. Jia, Y. Y. Cao, Z. N. Wang, Y. P. Wang, *Adv. Mater.* **2015**, *27*, 4622.

© 2020 Wiley-VCH GmbH

[19] Z. Y. Lei, P. Y. Wu, *Nat. Commun.* **2018**, *9*, 1.
[20] S. J. Park, M. Gazzola, K. S. Park, S. Park, V. Di Santo, E. L. Blevins, J. U. Lind, P. H. Campbell, S. Dauth, A. K. Capulli, F. S. Pasqualini, S. Ahn, A. Cho, H. Y. Yuan, B. M. Maoz, R. Vijaykumar, J. W. Choi, K. Deisseroth, G. V. Lauder, L. Mahadevan, K. K. Parker, *Science* **2016**, *353*, 158.
[21] J. W. Chen, F. K. C. Leung, M. C. A. Stuart, T. Kajitani, T. Fukushima, E. van der Giessen, B. Feringa, *Nat. Chem.* **2018**, *10*, 132.
[22] F. Lancia, A. Ryabchun, A. D. Nguindjel, S. Kwangmettatam, N. Katsonis, *Nat. Commun.* **2019**, *10*, 4819.
[23] S. M. Mirvakili, I. W. Hunter, *Adv. Mater.* **2018**, *30*, 1704407.
[24] J. A. Lv, Y. Y. Liu, J. Wei, E. Q. Chen, L. Qin, Y. L. Yu, *Nature* **2016**, *537*, 179.
[25] Y. Yang, Z. Pei, Z. Li, Y. Wei, Y. Ji, *J. Am. Chem. Soc.* **2016**, *138*, 2118.
[26] Z. Wang, H. Tian, Q. He, S. Cai, *ACS Appl. Mater. Interfaces* **2017**, *9*, 33119.
[27] R. R. Kohlmeyer, P. R. Buskohl, J. R. Deneault, M. F. Durstock, R. A. Vaia, J. Chen, *Adv. Mater.* **2014**, *26*, 8114.
[28] A. Oyefusi, J. Chen, *Angew. Chem., Int. Ed.* **2017**, *56*, 8250.
[29] Y. Y. Xiao, Z. C. Jiang, X. Tong, Y. Zhao, *Adv. Mater.* **2019**, *31*, 1903452.
[30] R. C. P. Verpaalen, M. P. da Cunha, T. A. P. Engels, M. G. Debije, A. Schenning, *Angew. Chem., Int. Ed.* **2020**, *59*, 4532.
[31] E. Mattia, S. Otto, *Nat. Nanotechnol.* **2015**, *10*, 111.
[32] J. Q. Liao, M. Yang, Z. Liu, H. L. Zhang, *J. Mater. Chem. A* **2019**, *7*, 2002.
[33] M. L. Du, L. H. Li, J. T. Zhang, K. X. Li, M. J. Cao, L. X. Mo, G. S. Hu, Y. J. Chen, H. F. Yu, H. Yang, *Liq. Cryst.* **2019**, *46*, 37.
[34] L. C. Liu, L. L. Rui, Y. Gao, W. A. Zhang, *Polym. Chem.* **2014**, *5*, 5453.
[35] C. Q. Qin, Y. Y. Feng, W. Luo, C. Cao, W. P. Hu, W. Feng, *J. Mater. Chem. A* **2015**, *3*, 16453.
[36] R. J. Dong, Y. Liu, Y. F. Zhou, D. Y. Yan, X. Y. Zhu, *Polym. Chem.* **2011**, *2*, 2771.
[37] S. Samai, C. Sapsanis, S. P. Patil, A. Ezzeddine, B. A. Moosa, H. Omran, A. H. Emwas, K. N. Salama, N. M. Khashab, *Soft Matter* **2016**, *12*, 2842.
[38] Y. Takashima, K. Yonekura, K. Koyanagi, K. Iwaso, M. Nakahata, H. Yamaguchi, A. Harada, *Macromolecules* **2017**, *50*, 4144.
[39] S. Hou, P. X. Ma, *Chem. Mater.* **2015**, *27*, 7627.
[40] F. D. Li, H. H. Hou, J. Yin, X. S. Jiang, *ACS Macro Lett.* **2017**, *6*, 848.
[41] S. M. Chin, C. V. Synatschke, S. P. Liu, R. J. Nap, N. A. Sather, Q. F. Wang, Z. Alvarez, A. N. Edelbrock, T. Fyrner, L. C. Palmer, I. Szleifer, M. O. de la Cruz, S. I. Stupp, *Nat. Commun.* **2018**, *9*, 1.
[42] Y. Y. Wang, Q. Q. Guo, G. H. Su, J. Cao, J. Z. Liu, X. X. Zhang, *Adv. Funct. Mater.* **2019**, *29*, 1906198.
[43] E. Borre, J. F. Stumbe, S. Bellemin-Laponnaz, M. Mauro, *Angew. Chem., Int. Ed.* **2016**, *55*, 1313.
[44] P. Cordier, F. Tournilhac, C. Soulie-Ziakovic, L. Leibler, *Nature* **2008**, *451*, 977.
[45] S. Y. Fu, H. Zhang, Y. Zhao, *J. Mater. Chem. C* **2016**, *4*, 4946.
[46] J. I. Mamiya, A. Yoshitake, M. Kondo, Y. Yu, T. Ikeda, *J. Mater. Chem.* **2008**, *18*, 63.
[47] Q. Y. Si, Y. Y. Feng, W. X. Yang, L. X. Fu, Q. H. Yan, L. Q. Dong, P. Long, W. Feng, *ACS Appl. Mater. Interfaces* **2018**, *10*, 29909.
[48] C. Q. Qin, Y. Y. Feng, H. R. An, J. K. Han, C. Cao, W. Feng, *ACS Appl. Mater. Interfaces* **2017**, *9*, 4066.
[49] A. V. Medvedev, E. B. Barmatov, A. S. Medvedev, V. P. Shibaev, S. A. Ivanov, M. Kozlovsky, J. Stumpe, *Macromolecules* **2005**, *38*, 2223.
[50] R. C. P. Verpaalen, M. G. Debije, C. M. Bastiaansen, H. Halilovic, T. A. P. Engels, A. Schenning, *J. Mater. Chem. A* **2018**, *6*, 17724.
[51] M. Zheng, T. J. Long, X. L. Chen, J. Q. Sun, *Chin. J. Polym. Sci.* **2019**, *37*, 52.
[52] G. ten Brinke, J. Ruokolainen, O. Ikkala, *Adv. Polym. Sci.* **2007**, *207*, 113.
[53] K. Aoki, M. Nakagawa, K. Ichimura, *J. Am. Chem. Soc.* **2000**, *122*, 10997.
[54] Y. Ni, X. Li, J. Hu, S. Huang, H. F. Yu, *Chem. Mater.* **2019**, *31*, 3388.
[55] Q. Zhang, C. Y. Shi, D. H. Qu, Y. T. Long, B. L. Feringa, H. Tian, *Sci. Adv.* **2018**, *4*, 8192.
[56] T. H. Zhao, Y. Wu, Y. D. Li, M. Wang, J. B. Zeng, *ACS Sustainable Chem. Eng.* **2017**, *5*, 1938.
[57] L. Liu, C. Pan, L. Q. Zhang, B. C. Guo, *Macromol. Rapid Commun.* **2016**, *37*, 1603.
[58] H. Z. Ying, Y. F. Zhang, J. J. Cheng, *Nat. Commun.* **2014**, *5*, 3218.
[59] J. X. Cui, D. Daniel, A. Grinthal, K. X. Lin, J. Aizenberg, *Nat. Mater.* **2015**, *14*, 790.
[60] M. Wang, B. P. Lin, H. Yang, *Nat. Commun.* **2016**, *7*, 1.
[61] O. M. Wani, R. Verpaalen, H. Zeng, A. Priimagi, A. Schenning, *Adv. Mater.* **2019**, *31*, 1805985.
[62] C. Lv, H. Xia, Q. Shi, G. Wang, Y. S. Wang, Q. D. Chen, Y. L. Zhang, L. Q. Liu, H. B. Sun, *Adv. Mater. Interfaces* **2017**, *4*, 1601002.

 © 2020 Wiley-VCH GmbH